

## Co-existing coupling schemes at high spin in $^{166}\text{Hf}$

D. Ringkjøbing Jensen<sup>1</sup>, J. Domscheit<sup>2</sup>, G.B. Hagemann<sup>1</sup>, M. Bergström<sup>1</sup>, B. Herskind<sup>1</sup>, B.S. Nielsen<sup>1</sup>, G. Sletten<sup>1</sup>, P.G. Varmette<sup>1</sup>, S. Törmänen<sup>1</sup>, H. Hübel<sup>2</sup>, W. Ma<sup>3</sup>, A. Bracco<sup>4</sup>, F. Camera<sup>4</sup>, F. Demaria<sup>4</sup>, S. Frattini<sup>4</sup>, B. Million<sup>4</sup>, D. Napoli<sup>5</sup>, A. Maj<sup>6</sup>, B.M. Nyakó<sup>7</sup>, D.T. Joss<sup>8,9</sup>, and M. Aiche<sup>10</sup>

<sup>1</sup> The Niels Bohr Institute, Blegdamsvej 17, DK-2100 Copenhagen Ø, Denmark

<sup>2</sup> Institut für Strahlen- und Kernphysik, University of Bonn, Germany

<sup>3</sup> Mississippi State University, Mississippi State, MS 39762, USA

<sup>4</sup> Dipartimento di Fisica, Università di Milano and INFN Milano, Italy

<sup>5</sup> Laboratori Nazionali Legnaro and INFN Padova, Italy

<sup>6</sup> Niewodniczanski Institute of Nuclear Physics, Krakow, Poland

<sup>7</sup> Institute of Nuclear Research (ATOMKI) H-4001 Debrecen, Hungary

<sup>8</sup> Oliver Lodge Laboratory, University of Liverpool, Liverpool, UK

<sup>9</sup> School of Sciences, Staffordshire University, College Road, Stoke-on-Trent, ST4 2DE, UK

<sup>10</sup> CENBG, University of Bordeaux I., Bordeaux-Gradignan, France

Received: 6 April 2000

Communicated by D. Schwalm

**Abstract.** The nucleus  $^{166}\text{Hf}$  has been populated by the reaction  $^{96}\text{Zr}(^{74}\text{Ge},4n)$  using a beam energy of 310 MeV.  $\gamma$ -rays were detected with the EUROBALL III detector array. Fourteen new normal-deformed rotational bands, of which six form coupled pairs, have been observed in  $^{166}\text{Hf}$ . Four previously known bands have been extended to considerably higher spin, and configurations of the new bands are proposed. Two different bands have been assigned configurations involving the same orbitals at high spin. The two coupling schemes, deformation and rotation alignment, are discussed in connection with this new observation, which calls for a formulation of co-existing coupling schemes in six-quasiparticle structures involving the same orbitals at high spin.

**PACS.** 21.10.-k Properties of nuclei; nuclear energy levels – 23.20.Lv Gamma transitions and level energies – 25.70.-z Low and intermediate energy heavy-ion reactions – 27.70.+q  $150 \leq A \leq 189$

### 1 Introduction

In the even-even nucleus,  $^{166}\text{Hf}$ , normal-deformed rotational bands are expected mainly to be built upon two- or four-quasiparticle excitations of the lowest orbitals close to the Fermi surface. For lower spin the configurations of these rotational bands are mainly two- and four-quasineutron states, whereas bands built upon proton excitations are expected at higher rotational frequency.

In the present experiment the level scheme of  $^{166}\text{Hf}$  [1] has been extended considerably. Eight new single and three coupled rotational bands have been observed. The four previously known bands in  $^{166}\text{Hf}$  have been extended to significantly higher spin. Spin and parity of the new bands have been determined by measuring angle-dependent intensity ( $I_\gamma(\theta)$ ) ratios using the method of directional correlation of decays from oriented nuclear states (DCO). In the present paper the configurations of the observed rotational bands are proposed and found to be in good agreement with the theoretical predictions based on Ultimate Cranker (UC) calculations [2]. The observed ro-

tational bands are found to represent many of the combinations of two- and four-quasineutron configurations made from the lowest single-quasineutron orbitals above the Fermi surface. Complete spectroscopy has therefore been approached within a region of  $\sim 1$  MeV above yrast.

Of special interest is one of the new coupled bands and one of the previously known, now extended, bands. At high spin the configurations of these two bands are proposed to involve the same orbitals. This observation is interpreted as a co-existence of the two different coupling schemes, deformation and rotation alignment. We believe that co-existing coupling schemes in six-quasiparticle structures involving the same orbitals at high spin are reported here for the first time. Together with this new observation another discovery has been made. In this specific coupled band the second quasineutron crossing (the BC crossing) is shifted towards higher rotational frequency compared to the BC crossings observed in other bands in  $^{166}\text{Hf}$ . This delay is probably caused by a combination of a deformation change and a neutron-proton interaction.

The proposed configurations of the new observed rotational bands in  $^{166}\text{Hf}$  will be presented and discussed. A more detailed discussion of deformation and rotation alignment is given.

## 2 Experiment and data analysis

High-spin states in  $^{166}\text{Hf}$  were populated in the  $^{96}\text{Zr}(^{74}\text{Ge},4n)$  reaction using a beam energy of 310 MeV provided by the XTU tandem accelerator and the linear accelerator ALPI at INFN in Legnaro, Italy. The target was a  $700\ \mu\text{g}/\text{cm}^2$  self-supporting Zr-target enriched to 85.25%.  $\gamma$ -rays were detected with the EUROBALL III spectrometer [3,4], which was equipped with 30 Tapered and 15 Cluster Ge-detectors in the forward and backward directions, respectively. The 26 Clover Ge-detectors were situated close to an angle of  $90^\circ$  relative to the beam axis. BGO-shields surrounded each type of detector. A total of  $3.96 \cdot 10^9$  coincidences with  $F \geq 5$  of unsuppressed Ge-detector events was measured. After presorting this resulted in  $2.93 \cdot 10^9$  three-,  $1.91 \cdot 10^9$  four- and  $1.0 \cdot 10^9$  five- and higher-fold coincidences of Compton-suppressed Ge-signals. The coincidences were sorted into a  $\gamma$ - $\gamma$ - $\gamma$  cube (3-D) and a  $\gamma$ - $\gamma$ - $\gamma$ - $\gamma$  hypercube (4-D) using Radware software [5]. The data in the cube and hypercube were analysed with the Radware programs Levit8r and Xm4dg, respectively.

### 2.1 DCO ratios

In order to determine spin and parity of the new observed rotational bands, the data was sorted into three gated  $\gamma$ - $\gamma$  matrices for each new band and analysed using the program Gf2 [5]. The experimental DCO ratios were obtained by measuring the intensities of the  $\gamma$ -rays at the angles  $\theta_1 \approx 90^\circ$  and  $\theta_2 \approx 154^\circ$  relative to the beam axis, where  $\theta_2$  is the average angle of the forward and backward detectors. The three types of matrices with different angle combinations were  $(x, y) = (\sim 154^\circ, \text{all angles})$ ,  $(x, y) = (\sim 90^\circ, \text{all angles})$  and  $(x, y) = (\sim 154^\circ, \sim 90^\circ)$ . The DCO ratio is defined as

$$R_{\text{DCO}} = \frac{I_{\theta_1}^{\gamma_2}(\text{gate}_{\theta_2}^{\gamma_1})}{I_{\theta_2}^{\gamma_2}(\text{gate}_{\theta_1}^{\gamma_1})}, \quad (1)$$

where  $I_{\theta_1}^{\gamma_2}(\text{gate}_{\theta_2}^{\gamma_1})$  is the intensity of the  $\gamma_2$ -ray at  $\theta_1$  in a spectrum gated by  $\gamma_1$  detected at  $\theta_2$  and  $I_{\theta_2}^{\gamma_2}(\text{gate}_{\theta_1}^{\gamma_1})$  is the intensity of the  $\gamma_2$ -ray at  $\theta_2$  in a spectrum gated by  $\gamma_1$  detected at  $\theta_1$ . The experimental DCO ratios were in all cases obtained from the  $(x, y) = (\sim 154^\circ, \sim 90^\circ)$  matrix. In this situation the values of  $R_{\text{DCO}}$  depend on the gating conditions and the expected values of  $R_{\text{DCO}}$  are indicated in table 1. Consistency with the data in the combination of the two first matrices, which have an expected smaller amplitude but higher statistics, were checked. Experimental DCO ratios of transitions with known multipolarity have been obtained and found to be in good agreement with the theoretical DCO ratios shown in table 1 [6,7].

**Table 1.** The expected DCO ratio of the first transition in a  $\gamma$ -cascade, where the gate is put on the second transition. If the gate or the transitions are interchanged, the DCO ratio is inverted.  $Q$  and  $D$  refer to quadrupole and dipole transitions, respectively.

$\gamma$ -cascade	$R_{\text{DCO}}$
$I \xrightarrow{Q} I-2 \xrightarrow{Q} I-4$	1.0
$I \xrightarrow{Q} I-2 \xrightarrow{D} I-3$	$\sim 0.6$
$I \xrightarrow{Q} I-2 \xrightarrow{D} I-2$	$\sim 1.0$
$I \xrightarrow{Q} I-2 \xrightarrow{Q} I-2$	$\sim 0.6$
$I \xrightarrow{D} I-1 \xrightarrow{D} I-2$	1.0
$I \xrightarrow{D} I-1 \xrightarrow{D} I-1$	$\sim 1.7$

### 2.2 B(M1)/B(E2) values

For coupled bands with connecting  $\Delta I = 1$  mixed  $M1/E2$  transitions the experimental values of  $B(M1, I \rightarrow I-1)/B(E2, I \rightarrow I-2)$  have been extracted from the expression

$$\frac{B(M1)}{B(E2)} = 0.693 \frac{T_{\gamma_1} E_{\gamma_2}^5}{T_{\gamma_2} E_{\gamma_1}^3} \frac{1}{1 + \delta^2}, \quad (2)$$

where  $\gamma_1$  and  $\gamma_2$  refer to the  $\Delta I = 1$  and  $\Delta I = 2$  transitions, respectively, with  $E_\gamma$  in MeV, and  $\delta^2 = T_{\gamma_1}(E2)/T_{\gamma_1}(M1)$ . The influence from the mixing ratio  $\delta$  can be estimated from the results of rigid-rotor calculations [8]. The correction is in general less than 10% and has therefore been neglected. The calculated  $B(M1)$  values are based on an extension of the geometrical model of ref. [9]

$$B(M1, I \rightarrow I-1) = \frac{3}{8\pi I^2} \left\{ \sqrt{I^2 - K^2} \left[ \sum_j (g_j - g_R) \Omega_j \right] - K \left[ \sum_j (g_j - g_R) i_j \right] \right\}^2 \mu_N^2. \quad (3)$$

The value used for the collective gyromagnetic ratio is  $g_R = 0.35$ . The intrinsic  $g$  factors,  $g_j$ , used for the different quasiparticle orbitals (see table 2) are A, B, C, D:  $-0.28$ ; E, F:  $0.25$ ; G, H:  $-0.61$ ; e, f:  $1.29$ ; g:  $0.76$ ; a, b:  $0.63$ ; k:  $1.35$ . The values of  $g_j$  have been calculated from the wave functions in [10]. For the aligned quasineutron pair (BC) a summed alignment of  $4.5\hbar$  together with  $K = 0$  has been used. The theoretical  $B(E2)$  values have been calculated according to the expression [8]

$$B(E2, I \rightarrow I-2) = \frac{5}{16\pi} Q_0^2 (IK20|I-2K)^2, \quad (4)$$

where  $Q_0$  is  $5.49b$  [11,12].

## 3 Experimental results

The nucleus  $^{166}\text{Hf}$  has been studied earlier by K.P. Blume *et al.* [1] using the reaction  $^{148}\text{Sm}(^{22}\text{Ne},4n)$ . In that experiment the yrast band of  $^{166}\text{Hf}$  was observed to spin  $34^+$ ,

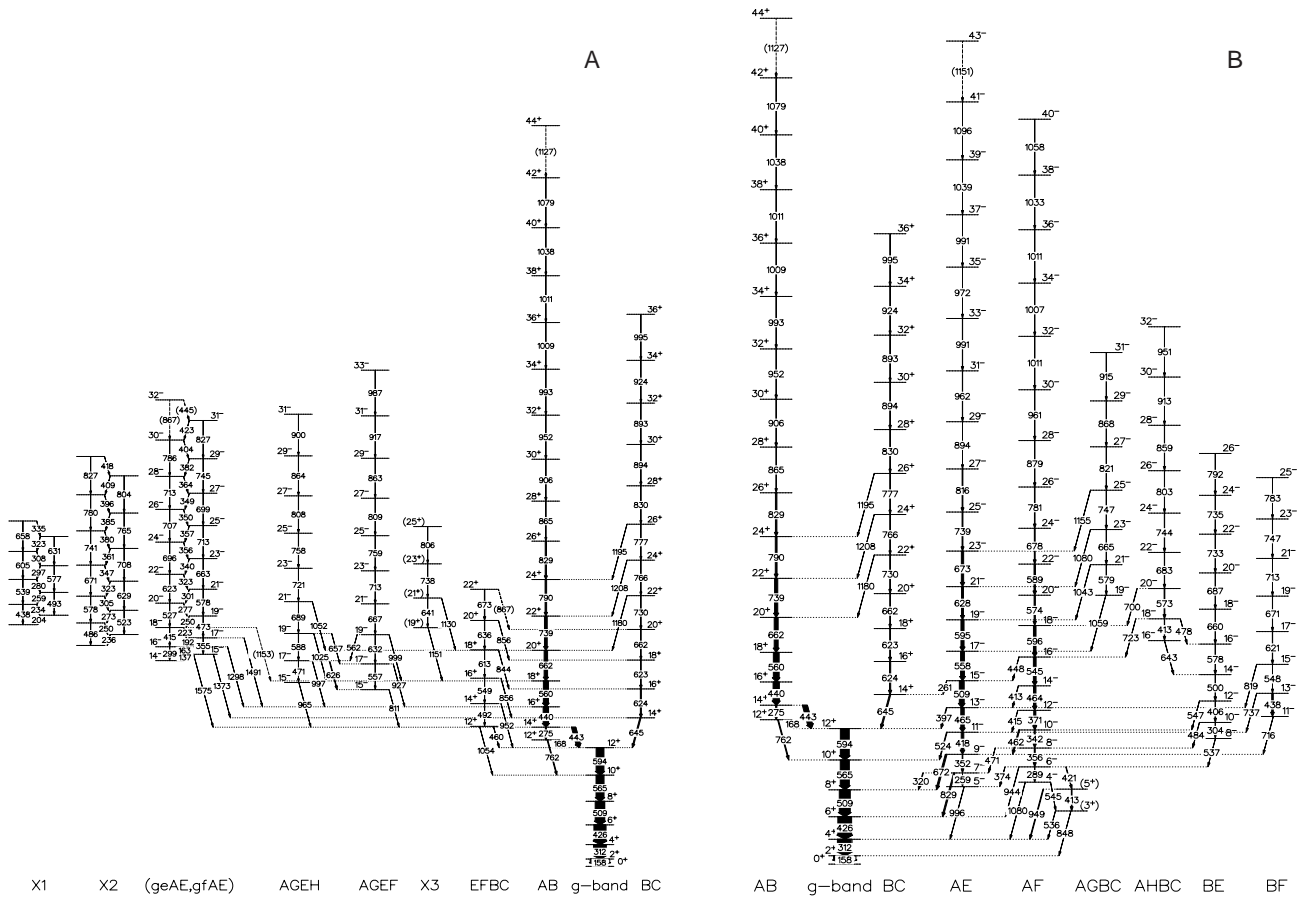


**Fig. 1.** Level scheme of  $^{166}\text{Hf}$ , part A and part B.

and the continuation of the ground-state band was found to reach the level  $22^+$ . Two other bands observed up to  $I^\pi = 33^-$  and  $32^-$ , respectively, have also been reported in ref. [1]. In the present work the level scheme of  $^{166}\text{Hf}$  has been extended considerably. Figures 1 A, B show the new level scheme of  $^{166}\text{Hf}$ . The configurations of the various bands are indicated in terms of letters, where upper case letters represent the quasineutron constituents of the configurations and lower case letters represent quasiprotons. This notation is explained in table 2 and the justification for the configuration assignment is given in section 5. The previously known bands are those labelled with the configurations AB, BC, AE and AF. In the present experiment eight new single and three coupled rotational bands have been found. Most of these new bands feed into either the yrast band (AB), the AE or the AF band except for two of the weaker coupled bands, X1 and X2, from which no decay-out transitions have been observed. The four formerly known bands have all been extended to higher spins, particularly the continuation of the ground-state band (BC), which has also been found to be connected with the yrast band via three interband transitions. The highest spin,  $I = 44\hbar$ , is reached in the yrast band (AB). Spectra documenting the coincidence relationships for the individual bands are shown in fig. 2.

## 4 Determination of spin and parity

Based on experimental DCO ratios of decay-out transitions from the various bands most of the new rotational bands have been assigned firm spin and parity by excluding multipole orders above 1 and 2 for magnetic and electric multipoles, respectively. Experimental DCO ratios are listed in table 3 [6, 7]. In some cases cross band transitions impose severe restrictions on relative spin and parities. The relative populations of the different bands have in certain cases been used for a less firm assignment of spin. The population pattern for bands of similar structure is strongly related to the excitation energy above yrast. The mutual consistency of the spin determination is illustrated in fig. 11. The individual quasiparticle assignments of the observed bands are discussed in section 5. Negative parity has been assigned to many of the bands, which is in good agreement with UC calculations. Only one of the new bands has been firmly assigned positive parity.

### 4.1 Positive-parity bands

#### 4.1.1 Band AB

The yrast band, AB, was known up to spin  $I = 34\hbar$  [1] and has now been extended by five new transitions to

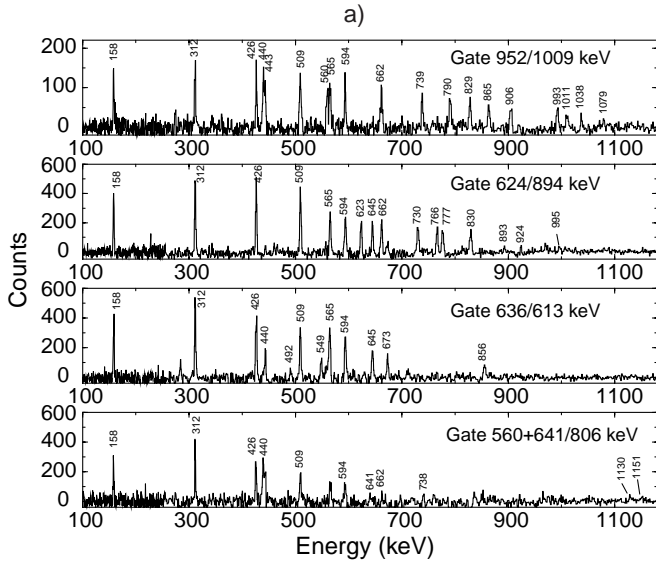


**Fig. 2.** Spectra of all the bands generated from the coincidence cube with the double gates indicated in each panel. Transitions belonging to or in coincidence with each band are labelled by their energies in keV. a) The figure shows from the upper to the lower panel the spectra of the yrast band (AB), band BC, band EFBC and band X3.

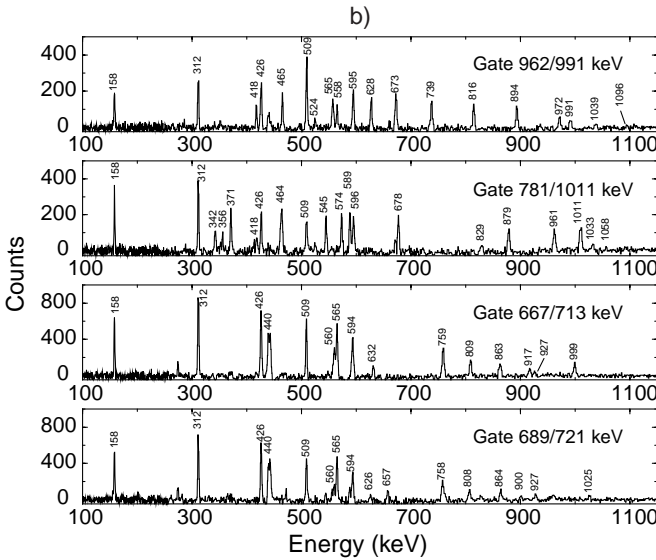


**Fig. 2.** b) From upper to lower panel the spectra of band AE, AF, AGEF and AGEH are indicated.

spin  $I = 44\hbar$ . The band has been assigned positive parity, and three transitions feeding into the ground-state band have been observed, namely 443 keV ( $14^+ \rightarrow 12^+$ ), 762 keV ( $12^+ \rightarrow 10^+$ ) and one new weak transition, 168 keV ( $12^+ \rightarrow 12^+$ ). The DCO ratios obtained in the present work for the 443 keV and 168 keV  $\gamma$ -rays are consistent with a stretched ( $I \rightarrow I - 2$ ) quadrupole and an unstretched quadrupole transition, respectively.

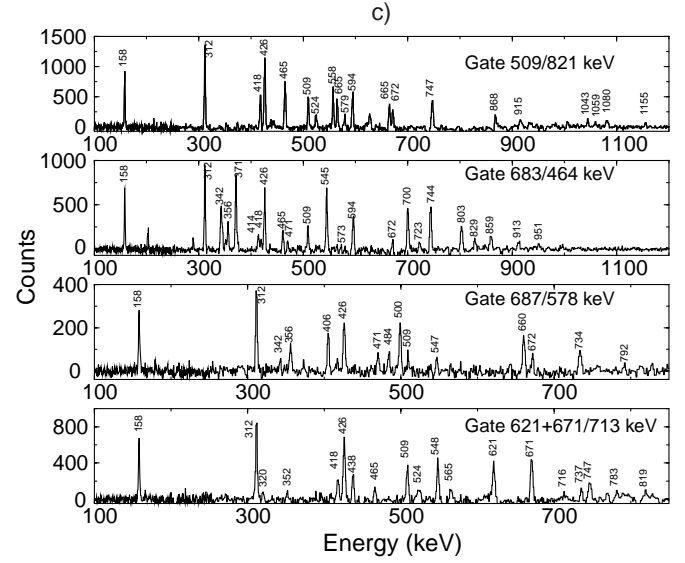


**Fig. 2.** c) From upper panel to lower panel the spectra of band AGBC, AHBC, BE and BF are shown.

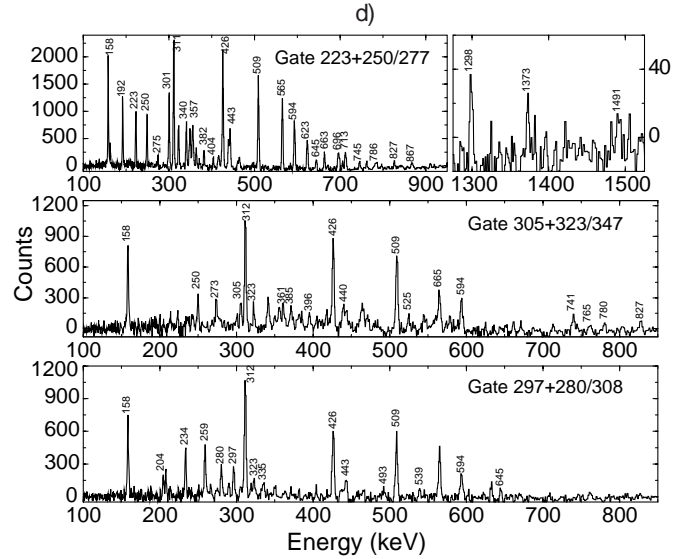


**Fig. 2.** d) From upper to lower panel the spectra of band (geAE, gfAE), X2 and X1 are indicated.

#### 4.1.2 Band BC

This band is the continuation of the ground-state band formerly known up to spin  $I = 22\hbar$  and assigned positive parity. The band has been extended by seven new transitions to  $36^+$  and is observed to interact with the yrast band via three interband transitions, 1195 keV ( $26^+ \rightarrow 24^+$ ), 1208 keV ( $24^+ \rightarrow 22^+$ ) and 1180 keV ( $22^+ \rightarrow 20^+$ ).

#### 4.1.3 Band EFBC

Each level belonging to the new band labelled EFBC decays into either the BC band or the ground-state band. Spin and parity of this band have been determined based

**Table 2.** Labels and alignments of theoretical Routhians.

Spherical shell model states	Nilsson orbitals	Labels		Alignment $i_x$	
		$\alpha = +1/2$	$\alpha = -1/2$	$\alpha = +1/2$	$\alpha = -1/2$
$\nu i_{13/2}$	$\nu[642]5/2^+$	A	B	5.5	4.5
$\nu i_{13/2}$	$\nu[651]3/2^+$	C	D	3	2
$\nu h_{9/2}$	$\nu[523]5/2^-$	E	F	2.5	2
$\nu f_{7/2}$	$\nu[521]3/2^-$	G	H	1.0	1.5
$\pi g_{7/2}$	$\pi[404]7/2^+$	a	b	0	0
$\pi i_{13/2}$	$\pi[660]1/2^+$	k	—	4	—
$\pi h_{11/2}$	$\pi[514]9/2^-$	e	f	1.5	1.5
$\pi h_{9/2}$	$\pi[541]1/2^-$	g	—	6	—

on DCO ratios of the transitions 856 keV ( $16^+ \rightarrow 14^+$ ) and 844 keV ( $18^+ \rightarrow 16^+$ ) both of stretched  $E2$  nature. Band EFBC has therefore been assigned positive parity and even spin.

#### 4.1.4 Band X3

The band X3 is relatively weak, and it has not been possible to obtain DCO ratios of the two transitions, 1130 keV and 1151 keV, depopulating this band to band AB. The tentative spin assignment is based on relative populations, and implies most likely positive parity, see section 5.1.4.

## 4.2 Negative-parity bands

### 4.2.1 Bands AE, AF

These two side bands were in ref. [1] assigned the two-quasineutron configurations AE and AF, respectively, corresponding to the Nilsson orbitals  $[642]5/2^+ \otimes [523]5/2^-$ . Several new transitions have been added to these two bands, so they now extend to spin  $I = 43\hbar$  and  $I = 40\hbar$ , respectively. In ref. [1] the parity of the two bands has been determined to be negative. A few new decay-out transitions feeding into the ground-state band have been found in the present data set. The DCO ratios of the 524 keV and 829 keV transitions clearly support the results of the previous work, in which the two  $\gamma$ -rays have been proposed to be stretched dipole transitions. The decay-out transitions of band AF to AE are of mixed  $M1/E2$  nature, and branching ratios have been analysed in ref. [1].

### 4.2.2 Bands BE, BF

A new group consisting of four rotational bands have been observed. These four bands (fig. 1 B most right) decay into either the AE or the AF band and have been assigned negative parity. Band BE, belonging to this group, decays into the AF band via three transitions 547 keV ( $12^- \rightarrow 10^-$ ), 484 keV ( $10^- \rightarrow 8^-$ ) and 537 keV ( $8^- \rightarrow 6^-$ ). Two transitions of energies 536 keV ( $3^+ \rightarrow 4^+$ ) and 545 keV ( $4^- \rightarrow 3^+$ ) located in the lower spin part of the AF band make it impossible to separate the 547 keV and 537 keV

transitions from the  $\gamma$ -rays of 545 keV and 536 keV by gating. Therefore spin and parity of the BE band have been determined solely on the basis of the DCO ratio of the 484 keV  $\gamma$ -ray, which is of stretched  $E2$  nature.

The determination of spin and parity of the band BF has been based on the DCO ratios of two transitions, 819 keV ( $15^- \rightarrow 13^-$ ) and 737 keV ( $13^- \rightarrow 11^-$ ) depopulating this band (BF  $\rightarrow$  AE). These two decay-out transitions have been found to be stretched quadrupoles, and the band BF has on this basis been assigned negative parity and odd spin.

### 4.2.3 Bands AGBC, AHBC

The two bands labelled AGBC and AHBC have been assigned negative parity and odd and even spin, respectively. The band AGBC decays into band AE through four transitions 1059 keV ( $19^- \rightarrow 17^-$ ), 1043 keV ( $21^- \rightarrow 19^-$ ), 1080 keV ( $23^- \rightarrow 21^-$ ) and 1155 keV ( $25^- \rightarrow 23^-$ ). DCO ratios of the three strongest of these transitions are consistent with stretched quadrupole character. The band AHBC is linked to both band AF via two transitions 723 keV ( $18^- \rightarrow 16^-$ ) and 700 keV ( $20^- \rightarrow 18^-$ ) and to band BE through the weak transitions 478 keV ( $18^- \rightarrow 16^-$ ) and 643 keV ( $16^- \rightarrow 14^-$ ). DCO ratios were obtained for the 700 keV and 723 keV  $\gamma$ -rays, which are also stretched quadrupole transitions.

### 4.2.4 Bands AGEF, AGEH

These bands are both connected to band AB through several transitions. Band AGEF is populated with higher intensity than band AGEH. The strongest decay-out transition at 999 keV is contaminated by another 999 keV transition in coincidence with itself and all transitions belonging to band AGEF, and no DCO ratio is determined. A connection between this second 999 keV transition and band AGEF has not been established.

Band AGEF is tied to band AGEH by a cross-band transition of 562 keV ( $19^- \rightarrow 17^-$ ). Two other transitions of energies 626 keV ( $17^- \rightarrow 15^-$ ) and 657 keV ( $19^- \rightarrow 17^-$ ) decaying from band AGEH to band AGEF have been observed. These interband transitions cause the

**Table 3.** Experimental DCO ratios.

Band	Transition		Gate		DCO ratio
	Energy (keV)	$I_i \rightarrow I_f$	Energy (keV)	$I_i \rightarrow I_f$	
AB	168	$12^+ \rightarrow 12^+$	440	$16^+ \rightarrow 14^+$	$1.50 \pm 0.15$
	443	$14^+ \rightarrow 12^+$	440	$16^+ \rightarrow 14^+$	$0.96 \pm 0.02$
AE	829	$7^- \rightarrow 6^+$	406	$12^- \rightarrow 10^-$	$1.77 \pm 0.23$
	524	$11^- \rightarrow 10^+$	628	$21^- \rightarrow 19^-$	$1.68 \pm 0.22$
AGBC	1043	$21^- \rightarrow 19^-$	665	$23^- \rightarrow 21^-$	$1.10 \pm 0.32$
	1059	$19^- \rightarrow 17^-$	579	$21^- \rightarrow 19^-$	$1.08 \pm 0.26$
	1080	$23^- \rightarrow 21^-$	747	$25^- \rightarrow 23^-$	$1.03 \pm 0.21$
AHBC	700	$20^- \rightarrow 18^-$	683	$22^- \rightarrow 20^-$	$0.99 \pm 0.10$
	723	$18^- \rightarrow 16^-$	573	$20^- \rightarrow 18^-$	$1.04 \pm 0.17$
BF	737	$13^- \rightarrow 11^-$	548	$15^- \rightarrow 13^-$	$0.96 \pm 0.08$
	819	$15^- \rightarrow 13^-$	747	$23^- \rightarrow 21^-$	$1.10 \pm 0.20$
BE	484	$10^- \rightarrow 8^-$	406	$12^- \rightarrow 10^-$	$0.98 \pm 0.08$
AGEH	1025	$19^- \rightarrow 18^+$	689	$21^- \rightarrow 19^-$	$1.41 \pm 0.27$
	1025	$19^- \rightarrow 18^+$	721	$23^- \rightarrow 21^-$	$1.59 \pm 0.43$
geAE	1298	$16^- \rightarrow 16^+$	223	$18^- \rightarrow 17^-$	$0.47 \pm 0.17$
and	1298	$16^- \rightarrow 16^+$	440	$16^+ \rightarrow 14^+$	$1.01 \pm 0.22$
gfAE	1491	$17^- \rightarrow 16^+$	223	$18^- \rightarrow 17^-$	$0.86 \pm 0.22$
EFBC	856	$16^+ \rightarrow 14^+$	613	$18^+ \rightarrow 16^+$	$0.82 \pm 0.29$
	844	$18^+ \rightarrow 16^+$	636	$20^+ \rightarrow 18^+$	$0.89 \pm 0.25$

two bands to have the same spin and parity disregarding  $\gamma$ -rays of electric and magnetic multipole order higher than 2 and 1, respectively. Spin and parity of these two bands have consequently been determined on the basis of the DCO ratios of the weak 1025 keV transition, consistent with stretched dipole character, connecting band AGEH to band AB. DCO ratios of all other decay-out transitions could not be obtained. Furthermore, the intensities of band AGEF and AGEH compared to those of band AB, AE and AF agree with their relative excitation. Therefore band AGEF and AGEH have both been assigned odd spin. Negative parity is chosen assuming that  $E1$  decay is more likely than  $M1$  decay.

#### 4.2.5 Band (geAE, gfAE)

Three coupled bands were observed, but only one of them, band (geAE, gfAE), has been linked to bands AB and BC via five transitions of energies 1153 keV ( $18^- \rightarrow 18^+$ ), 1491 keV ( $17^- \rightarrow 16^+$ ), 1373 keV ( $15^- \rightarrow 14^+$ ), 1575 keV ( $15^- \rightarrow 14^+$ ) and 1298 keV ( $16^- \rightarrow 16^+$ ). DCO ratios have been determined for the 1298 keV and 1491 keV  $\gamma$ -rays to be of unstretched dipole and stretched dipole character, respectively. Consequently band (geAE, gfAE) has been assigned negative parity assuming that  $E1$  is more likely than  $M1$  nature for these high energies.

#### 4.3 Bands X1, X2

Since no decay-out transitions have been observed from bands X1 and X2, spin and parity of these two coupled bands could not be determined. They both feed into band AB around spin  $16^+$ , see fig. 2d).

## 5 Identification of configurations

Table 2 lists the labelling and the alignments of the quasi-particles and related orbitals closest to the Fermi surface. Upper case letters represent quasineutrons and lower case letters quasiprotons. Each letter corresponds to a state described by a certain combination of the signature and parity quantum numbers. This table also shows the corresponding shell model states and asymptotic Nilsson labels at  $\hbar\omega = 0$  MeV. Theoretical Routhians of quasineutrons and quasiprotons are shown in figs. 3 and 4.

Some of the possible four-quasiparticle excitations are very similar in structure. In assigning configurations we have in such cases chosen to follow the order of excitation energy calculated by UC.

Figures 5 and 6 show the excitation energies of the positive- and negative-parity bands observed in  $^{166}\text{Hf}$  relative to a rigid-rotor reference  $A \cdot I(I+1)$ . In order to get a convenient scale,  $A$  was chosen to be 8 keV. In figs. 7 and 8 the experimental alignments of positive- and negative-parity bands are indicated as a function of rotational frequency, respectively. The reference parameters used are  $\mathcal{J}^{(0)} = 35 \text{ MeV}^{-1} \hbar^2$  and  $\mathcal{J}^{(1)} = 40 \text{ MeV}^{-3} \hbar^4$ . The experimental alignments of the two coupled bands, X1 and X2, of which firm spin and parity have not been determined, are not depicted in these figures. Quasiparticle assignments are based on observed alignments and crossings expected at characteristic frequencies. The first two neutron crossings are AB ( $\hbar\omega \approx 0.25$  MeV) and BC ( $\hbar\omega \approx 0.30$  MeV). The first proton crossings are expected at  $\hbar\omega \geq 0.42$  MeV. (See fig. 4.) It appears that considerable mixing of the available four-quasiparticle structures built on A, B, C, D, E and F exists. The assignments are therefore not firm in the high spin region concerning the quasineutrons, whereas the proton assignment at the

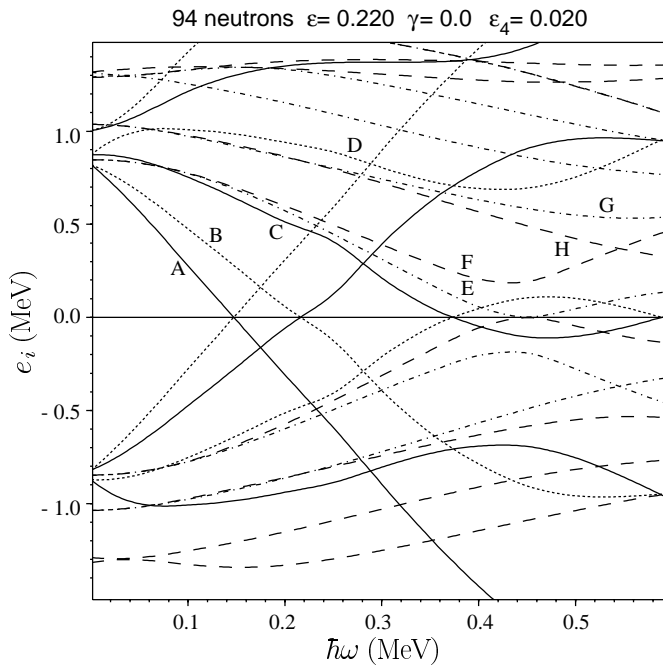


Fig. 3. Theoretical Routhians of quasineutrons.

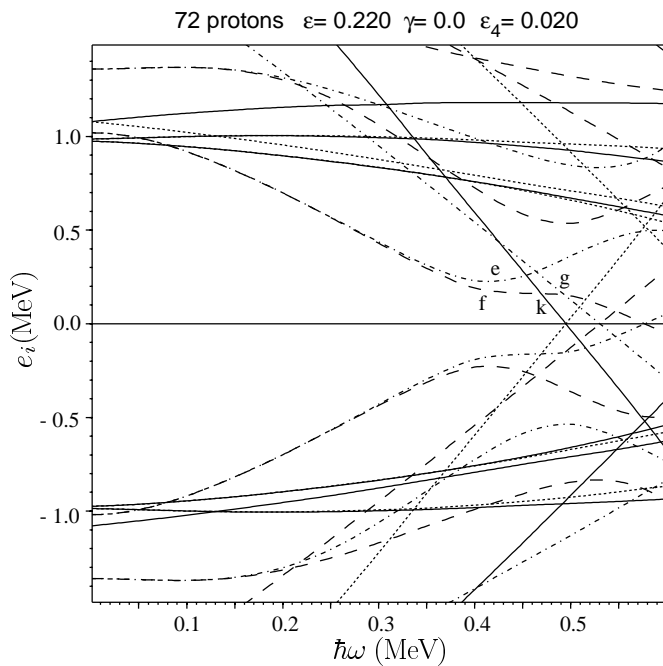


Fig. 4. Theoretical Routhians of quasiprotons.

highest frequencies is considered reliable. The configuration assignment for one of the new coupled bands has also been based on comparison between experimental and calculated  $B(M1)/B(E2)$  values.

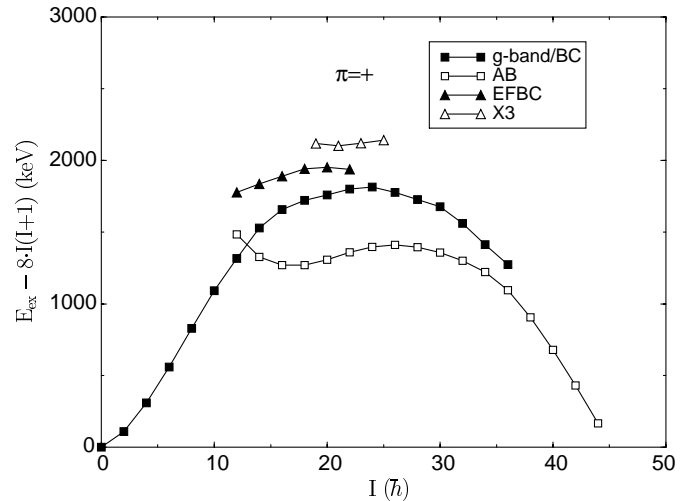


Fig. 5. Excitation energies of positive-parity bands in  $^{166}\text{Hf}$  as a function of spin relative to a rigid-rotor reference.

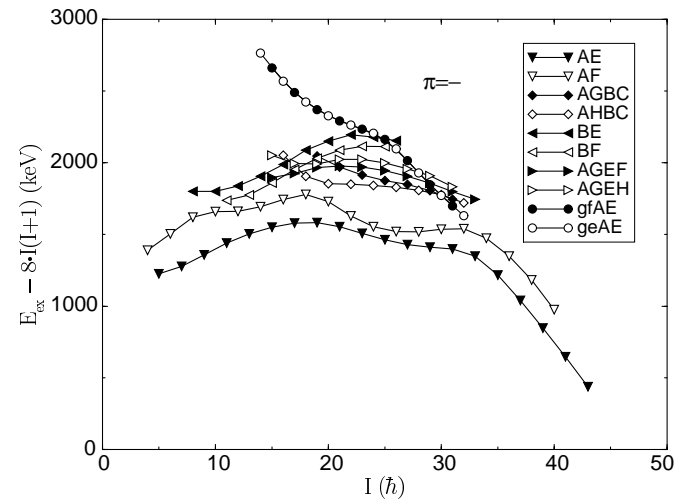
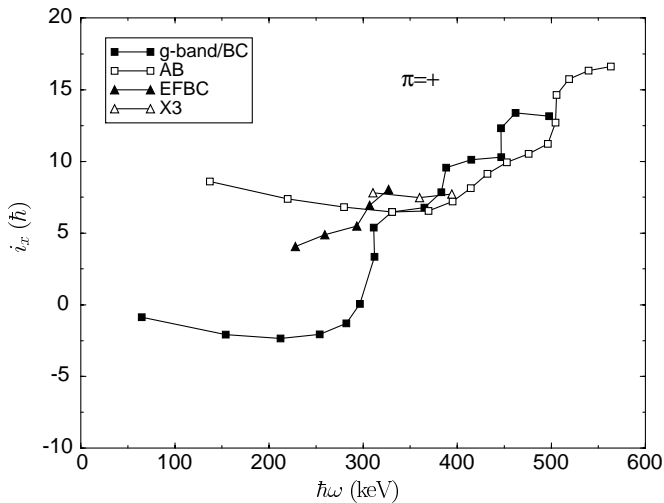


Fig. 6. Excitation energies of negative-parity bands in  $^{166}\text{Hf}$  as a function of spin relative to a rigid-rotor reference.

## 5.1 Positive-parity bands

### 5.1.1 Band AB

This band is yrast above  $I = 14\hbar$  and has earlier been assigned the two-quasineutron configuration AB corresponding to the Nilsson orbital  $[642]5/2^+$ . The alignment gain expected from the decoupling of the first pair of  $i_{13/2}$  quasineutrons is  $\sim 9.5\hbar$ , based on CSM calculations [1]. This is in good agreement with the alignment gain of  $\sim 10\hbar$  observed at  $\hbar\omega \approx 0.25$  MeV in this band relative to the g-band, see fig. 7. A gradual alignment gain of  $\sim 4\hbar$  in the frequency range between  $\hbar\omega \approx 0.35$  MeV and  $\hbar\omega \approx 0.49$  MeV is observed. This increase is probably due to an alignment of the neutron pair, CD or EF. The CD and EF crossings can be isolated in the odd neighbours,  $^{165,167}\text{Hf}$  [13,14], where the ABC and the EAB band will have the CD and EF crossings blocked, respectively. In both nuclei [13,14] the ABC band shows no crossings be-



**Fig. 7.** Alignments of positive-parity bands in  $^{166}\text{Hf}$  as a function of rotational frequency.

fore a suggested proton crossing sets in at  $\hbar\omega \approx 0.5$  MeV, which seems to indicate that the EF crossing should be barely visible in  $^{166}\text{Hf}$  as well. The CD crossing is clearly observed [13] at  $\hbar\omega \approx 0.41$  MeV in the ABE and ABF bands in  $^{165}\text{Hf}$ , whereas the same crossings in  $^{167}\text{Hf}$  appear as a gradual alignment gain corresponding presumably to a larger interaction in the frequency range between  $\hbar\omega \approx 0.3$  and  $\hbar\omega \approx 0.45$  MeV. From this comparison the second crossing in band AB should therefore be interpreted as the CD crossing. The EF crossing is probably very close in frequency, and actually necessary to be taken into consideration for an understanding of all three positive-parity bands with even spin ( $\alpha = 0$ ) in  $^{166}\text{Hf}$ , cf. the following subsections. The large alignment gain of  $\sim 6\hbar$  observed at  $\hbar\omega \approx 0.5$  MeV probably has to involve quasiprotons, since it is observed as a general phenomenon in all the bands, which have been extended high enough in spin. The large alignment gain cannot be explained by excitation of the e and f quasiprotons alone, based on the  $[514]9/2^-$  orbital. The g quasiproton based on the  $[541]1/2^-$  orbital, which has a large alignment and actually crosses the e orbital at  $\hbar\omega \approx 0.48$  MeV, must be involved as well. (See fig. 4.) Therefore, at high spin band AB is assigned as ABCDfg with the qualification that some mixture with ABEFfg probably is present.

### 5.1.2 Band BC

The g-band extends after the sharp AB crossing by the yrast band into a rather large alignment gain at  $\hbar\omega \approx 0.3$  MeV, which can be interpreted as the expected BC crossing. The BC band experiences two additional crossings with moderate alignment gain, and we suggest that the AD and EF quasineutrons are involved successively. There is a pronounced cross band transition strength to band AB for spins  $I = 22 - 26\hbar$ , with  $B(E2)_{\text{out}}/B(E2)_{\text{in}} \sim 0.05$ , which reveals some mixing between the bands. The band is weaker populated than band AB, and there-

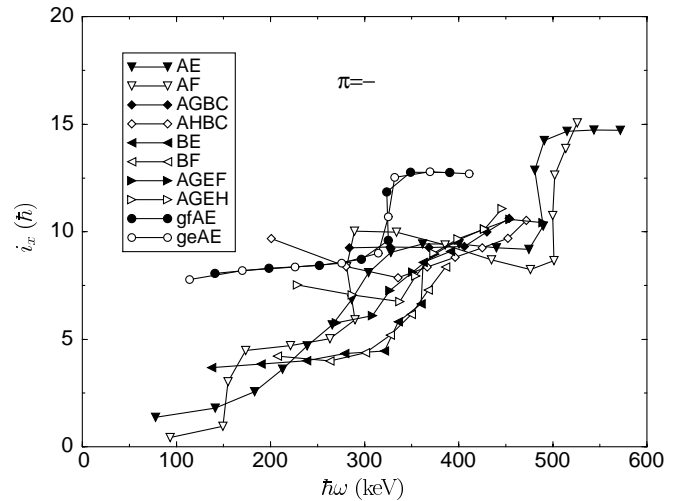


**Fig. 8.** Alignments of negative-parity bands in  $^{166}\text{Hf}$  as a function of rotational frequency.

fore not extended very high in spin. There are some extra transitions observed feeding in above  $I = 30\hbar$ , but no specific band structure could be identified.

### 5.1.3 Band EFBC

The third band with  $(\pi, \alpha) = (+, 0)$  is higher in excitation and not extending very high in spin. It has a gradual alignment gain around the BC frequency, and shows a rather strong decay branching to band BC with a  $B(E2)_{\text{out}}/B(E2)_{\text{in}} \sim 0.09$ . A possible candidate is EFBC, which could be consistent with its mixing into BC and therefore explain the decay pattern. Other low excitations with  $(\pi, \alpha) = (+, 0)$  are EHAB and FGAB, which are disregarded since they should have a larger alignment than AB above the AB crossing frequency of 0.25 MeV.

### 5.1.4 Band X3

This band has spin assignment based on its population. If the parity was negative the energy of the state with spin 23 would be within 5 keV from the same state in band BFAD. The two bands do not interact, and we therefore prefer positive parity for band X3, which implies that the decay consists of unstretched quadrupole transitions possibly mixed with  $M1$ . For a band with this signature the only possible decay is to the yrast band with opposite signature. The band is short, with large alignment, and we tentatively assign it to the lowest expected structure with  $(\pi, \alpha) = (+, 1)$ , ABEG, which agrees with its alignment.

## 5.2 Negative-parity bands

### 5.2.1 Bands AE, AF

Bands AE and AF have both been observed in earlier experiments [1]. The configurations AE and AF,  $[642]5/2^+ \otimes$



$[523]5/2^-$ , correspond to the two lowest two-quasineutron configurations of negative parity. Since the A quasineutron is contained in the configurations, a BC crossing is expected to be observed in both bands. An increase in the alignment of  $\sim 5\hbar$  observed at  $\hbar\omega \approx 0.28$  MeV in band AF is identified as the expected BC crossing. In band AE the BC crossing is seen as a gradual increase in alignment from  $\hbar\omega \approx 0.18$  MeV to  $\hbar\omega \approx 0.36$  MeV. This effect could be due to the influence of low-lying octupole vibrational bands in these two negative-parity bands [1]. In the present work both bands have been extended to higher spin and new alignments around  $\sim 6\hbar$  have been observed at  $\hbar\omega \approx 0.50$  MeV. Due to this rather large alignment gain the g proton, originating from  $[541]1/2^-$ , must be excited at high spin in both bands. Following the same arguments as for band AB, band AE and AF have at high spin been assigned the configurations AEBCfg and AFBCfg, respectively.

### 5.2.2 Bands BE, BF

The relatively low alignment at low spin of both of these two bands suggests that they are two-quasiparticle configurations, see fig. 8. Their excitation energies are just above the AE and AF configurations (fig. 6) and possible two-quasineutron configurations could therefore be BE and BF or AG and AH. At a rotational frequency of  $\hbar\omega \approx 0.32$  MeV an increase in alignment is observed. The BC crossing in band AF occurs at  $\hbar\omega \approx 0.28$  MeV. The upbend observed in the bands labelled BE and BF could consequently be caused by an AD crossing, which is expected at a little higher rotational frequency than the BC crossing, see fig. 3. Based on these observations the two bands have been assigned the configurations BE and BF. It should be noticed that the excitation energy of band BE is higher than that of band BF (see fig. 6). According to the theoretical calculations shown in fig. 3 the E orbital has lower excitation energy than the F orbital.

### 5.2.3 Bands AGBC, AHBC

The two-quasineutron configurations AG and AH are expected to have almost the same excitation energy as the BE and BF configurations. Therefore it is likely that bands built upon excitations to the AG and AH orbitals should also be found. However, the bands labelled AGBC and AHBC have a rather large alignment, which suggests that these bands are four-quasineutron structures. These two bands are assigned to the continuation of the AG and AH configurations into AGBC and AHBC. Due to mixing of AGBC with AEBC and AHBC with AFBC the two bands lose population and have not been observed as the two-quasineutron configurations AG and AH.

### 5.2.4 Bands AGEF, AGEH

These two bands have been assigned the same spin and parity. Three transitions of almost the same energy have

been observed in both bands from spin  $23^-$  to  $29^-$ , but without doubt two distinct bands have really been found, see fig. 2b). It is difficult to assign firm configurations to these bands, but possible candidates could be AGEF and AGEH taking into account that the bands are very similar and interact at the lowest spin. The excitation energy of band AGEH is a little higher than that of band AGEF. This agrees with the theoretical calculations, where the F quasineutron has a lower energy than the H quasineutron.

### 5.2.5 Band (geAE, gfAE)

Strong  $M1$  interband transitions have been observed between the two bands, which constitute the coupled band labelled (geAE, gfAE). The relatively large alignment and excitation energy (see figs. 6 and 8) at spin  $20^-$  suggest that this band is a four quasiparticle structure, probably also involving quasiprotons. A very sharp alignment is seen at a frequency of  $\hbar\omega \approx 0.33$  MeV, which is most likely a BC crossing. An AB crossing at  $\hbar\omega \approx 0.25$  MeV is clearly not observed in this band. The BC crossing is, on the other hand, shifted approximately 50 keV towards higher rotational frequency compared to the same crossing in band AF. This observation will be discussed below. Due to the fact that a BC crossing is observed the configuration of band (geAE, gfAE) must contain the A quasineutron. The other quasineutrons could therefore be D, E, F, G or H. The lowest combination of one of these with A is AE. The quasiprotons having the lowest energies are e, f and g, and are all of negative parity. A good candidate for the configuration is therefore  $\nu([642]5/2^+, [523]5/2^-) \otimes \pi([541]1/2^-, [514]9/2^-)$ , with different possibilities of the  $K$  quantum number. Another possibility, in which E is exchanged with G, could be  $\nu([642]5/2^+, [521]3/2^-) \otimes \pi([541]1/2^-, [514]9/2^-)$ . Figure 9 shows the experimental  $B(M1)/B(E2)$  values of band (geAE, gfAE) as a function of spin together with some relevant theoretical  $B(M1)/B(E2)$  values. Accordingly the configuration of band (geAE, gfAE) is proposed to be  $\nu([642]5/2^+, [523]5/2^-) \otimes \pi([541]1/2^-, [514]9/2^-)$  coupling to  $K^\pi = 10^-$ . The agreement is striking also above  $I = 23^-$ , where the BC crossing has been included.

The other possible configuration, where the same orbitals couple to  $K^\pi = 9^-$  has theoretical  $B(M1)/B(E2)$  values, which are lower at high spin than the  $K^\pi = 10^-$  configuration. If the E quasineutron is interchanged with F, and simultaneously the e proton with f, corresponding to the configuration (gfAF, geAF), the expected excitation energy becomes a little higher. The theoretical  $B(M1)/B(E2)$  values for this configuration are identical to those of (geAE, gfAE). If only E is interchanged with G or F with H, corresponding to the configurations (geAG, gfAG) or (gfAH, geAH), the theoretical  $B(M1)/B(E2)$  values become too small. The  $\alpha = +1/2$  part of the proton orbital  $[660]1/2^+$ , labelled k, is close to the Fermi surface as well, but  $B(M1)/B(E2)$  values of configurations involving this orbital together with  $[404]7/2^+$  are too low compared to the experimental values.

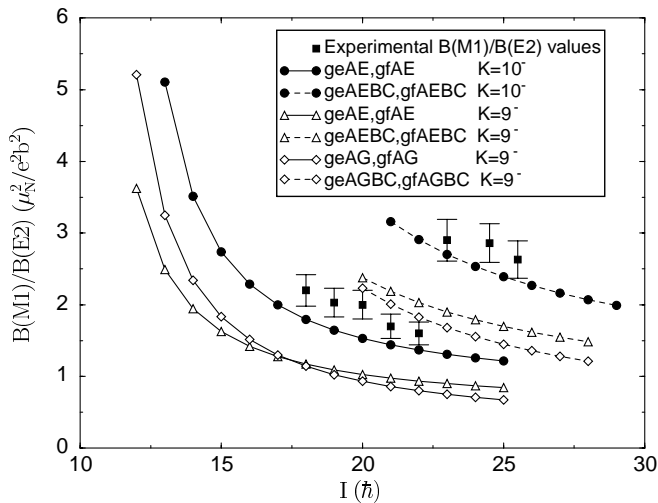


**Fig. 9.** Experimental  $B(M1)/B(E2)$  values of band (geAE, gfAE). The experimental data point placed at spin 24.5 has been measured using the summed intensity of the 357 keV ( $25^- \rightarrow 24^-$ ) and 356 keV ( $24^- \rightarrow 23^-$ ) transitions and the summed intensity of the 713 ( $25^- \rightarrow 23^-$ ) and 696 keV ( $24^- \rightarrow 22^-$ ) transitions. The last experimental data point placed at spin 25.5 was obtained using the summed intensity of the 349 keV ( $27^- \rightarrow 26^-$ ) and 350 keV ( $26^- \rightarrow 25^-$ ) transitions and the summed intensity of the 699 ( $27^- \rightarrow 25^-$ ) and 707 keV ( $26^- \rightarrow 24^-$ ) transitions. Theoretical  $B(M1)/B(E2)$  values for relevant configurations are indicated.

The delay of  $\sim 0.03$  MeV in the BC crossing frequency in band (geAE, gfAE) is consistent with a similar observation for a BC crossing in another band involving both the g quasiproton and the A quasineutron, namely the band gA in  $^{162}\text{Tm}$  [15]. The effect may be traced in a combination of proton-neutron interaction and increased deformation. This observation is supporting evidence of the g quasiproton being a part of the configuration of band (geAE, gfAE).

Based on the arguments mentioned above the final choice of configuration of band (geAE, gfAE) is settled on (geAE, gfAE), which has the lowest excitation energy of all candidates.

Band (geAE, gfAE) has been assigned  $K^\pi = 10^-$ . Five decay-out transitions depopulate the band around spin 16 to the AB band ( $K = 0$ ), and the lowest spin observed is  $I = 14\hbar$ . Due to these competing decay-out transitions the band head is not observed.  $B(E1)$  values of the 1491 keV, 1298 keV and 1373 keV decay-out transitions have been estimated to be  $7.9 \cdot 10^{-6}$ ,  $2.8 \cdot 10^{-5}$  and  $3.9 \cdot 10^{-5}$   $e^2 \text{ fm}^2$ , respectively, from observed out-of-band to in-band branching ratios based on an assumed quadrupole moment of 5.5 eb for the in-band  $E2$  transitions and observed  $B(M1)/B(E2)$  values. The  $B(M1)/B(E2)$  values were extrapolated to lower spin values than observed in agreement with the theoretical curve for the assigned configuration. The observed  $B(E1)$  values for transitions with  $\Delta K = 10$  show only little hindrance relative to observed  $K$ -allowed transitions, for which an effective reduction of  $10^4$  are customary relative to a standard single particle

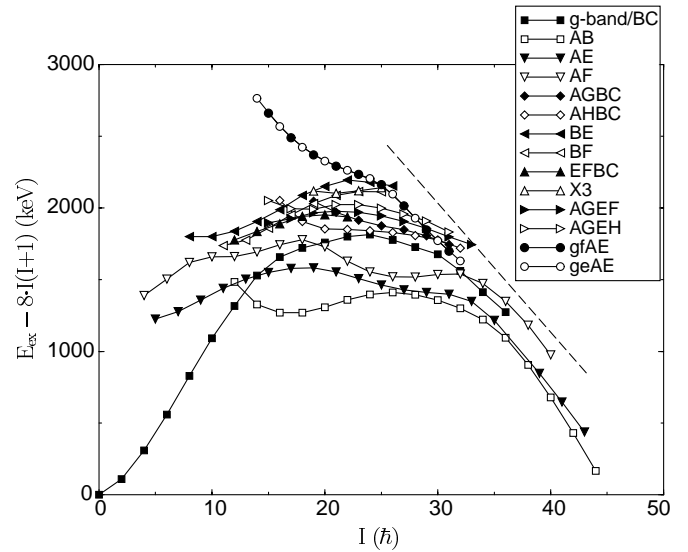


**Fig. 10.** Excitation energies of bands in  $^{166}\text{Hf}$  as a function of spin relative to a rigid-rotor reference.

unit of  $1.95 e^2 \text{ fm}^2$ . One could maybe find an explanation for this in the character of the constituent orbitals of band (geAE, gfAE), where the  $\pi[541]1/2^-$  and  $\nu[642]5/2^+$  orbitals both have large alignments, introducing a distribution in  $K$  around  $K = 10$  together with a distribution around  $K = 0$  for the AB band.

## 6 Discussion

### 6.1 Complete spectroscopy

Figure 10 shows the excitation energies of all the rotational bands found in  $^{166}\text{Hf}$  as a function of spin, relative to a rigid-rotor reference, except for the bands X1 and X2. The experiment has resulted in a multitude of band structures, which concentrate in a region of  $I \sim 20\text{--}30\hbar$ . There seems to be an upper limit (indicated by the dashed line) over which no rotational bands are observed. In general the level density is expected to increase with the distance from the yrast line, and discrete rotational bands in the region of high level density will be populated with smaller relative intensity, and therefore more difficult to detect. Figure 11 shows the intensities of bands in  $^{166}\text{Hf}$  as a function of excitation energy. The boundary limiting the observation of bands may be determined by the onset of quasiproton excitations, which is indeed expected, and actually found, at the highest spins of bands AB, AE, and AF. Quasiprotons are also excited in the coupled band (geAE, gfAE) at moderate spins, close to the boundary.

The spectrum of four-quasiparticle bands within the boundary is composed by combinations within the quasineutrons, A, B, C, D with positive parity and E, F and G, H with negative parity, respectively. Although the individual assignments of quasineutrons to the observed bands are not all unambiguous, the general structure can certainly be considered reliable. Within an excitation energy of around 1 MeV above yrast we expect

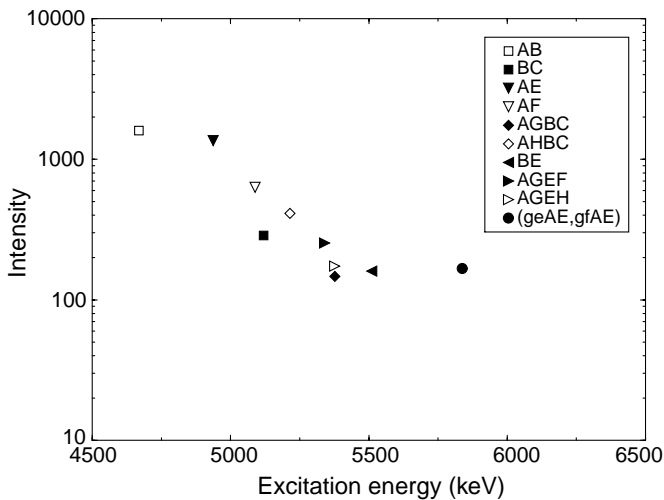


**Fig. 11.** Band intensities. In bands assigned even spin the band intensity has been obtained as the intensity of the transition from spin 22 to 20. In bands assigned odd spin the band intensity was obtained as the average intensity of the transitions from spin 23 to 21 and from spin 21 to 19. Intensities of bands BF, EFBC and X3 could not be determined.

from UC calculations 8 and 10 four-quasineutron bands with positive and negative parity, respectively, which can be compared to the experimental spectrum of 4 and 8 positive- and negative-parity bands. It should be emphasised that included in these 18 expected bands, are three bands, AGEF, AGEH and EFBC, with calculated excitation energies above 1 MeV, but observed below. These 3 bands are therefore added to the group of expected bands. Expressed as simple fractions the completeness is therefore approached by 50 and 80% for positive and negative parity, respectively, in this region. Similar observations in  $^{164}\text{Yb}$  at slightly lower spin are in [16] compared to UC calculations of the total expected spectrum of bands.

We note in this connection that the missing positive-parity bands could possibly be explained by the role of the yrast band being also of positive parity, which might cause the direct population from higher energy to compete more favourably. The missing positive-parity bands are in particular those calculated with odd spin. For the negative-parity bands one could add that two particular bands, assigned as AEGF and AEGH, are observed somewhat lower in excitation than calculated. They comprise the only four-quasiparticle bands with 3 negative-parity quasineutrons, which might impose a systematic effect on the excitation energies possibly traced in a changed pairing that is not treated self-consistently in the calculations for the individual structures.

## 6.2 Rotation and deformation alignment

The three lowest bands AB, AE and AF have all been extended quite high in spin. A large alignment gain of  $\Delta i_x \geq 6\hbar$  is observed at a rotational frequency  $\hbar\omega \approx 0.5\text{ MeV}$  in all of them. Due to the blocking of available

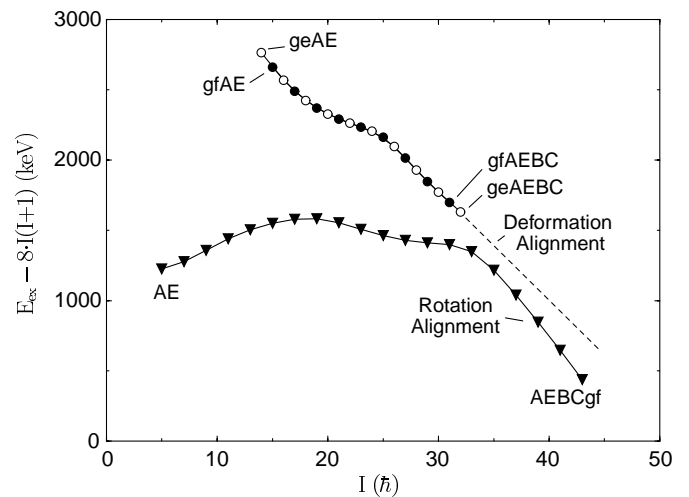


**Fig. 12.** Excitation energies of bands AE, gfAE and geAE in  $^{166}\text{Hf}$  as a function of spin relative to a rigid-rotor reference.

quasineutrons, this common alignment is interpreted as caused by quasiprotons. Instead of regular breaking of the lowest pair of  $h_{11/2}$  quasiprotons, which only produce an alignment gain of  $\Delta i_x \sim 2\hbar$ , a mixed crossing involving  $h_{11/2}, \alpha = -1/2$  (f) and  $h_{9/2}, \alpha = +1/2$  (g) must be responsible for the large alignment gain, in accordance with cranking calculations (UC). The  $h_{9/2}$  quasiproton corresponds at low frequency to the strongly shape-driving Nilsson orbital,  $[541]1/2^+$ , (see table 2 and fig. 4). The lowest negative-parity band, AE, which exhibits a BC crossing at  $\hbar\omega \approx 0.3\text{ MeV}$  develops into AEBCgf at  $I \sim 33\hbar$ .

The strongly coupled band with the two signatures labelled as geAE and gfAE has, from DCO ratios for its decay to the g- and AB band at spin 14-18 $\hbar$ , been assigned firm spin and negative parity. Its large alignment, lack of AB crossing, but clear BC crossing, together with a comparison of experimental and calculated  $B(M1)/B(E2)$  values impose severe constraints on the involved four-quasiparticle configurations. The only possible configuration is the AE quasineutrons ( $[642]5/2^+$  and  $[523]5/2^-$ ) coupled to the quasiprotons,  $h_{11/2}[514]9/2^-$  and  $h_{9/2}[541]1/2^-$  in their high- $K$  coupling mode to  $K^\pi = 5^-$ , with a total  $K^\pi = 10^-$ , as documented in section 5.2.5. The two signature partners are comprised by the orbital with the smallest signature splitting,  $h_{11/2}[514]9/2^-$ . The band changes into a six-quasiparticle structure at the BC crossing at  $\hbar\omega \approx 0.33\text{ MeV}$ .

Therefore, the coupled band and the negative-parity band, AE, are both of six-quasiparticle nature at their highest spins, where they appear to have identical quasiparticles involved, namely gf AE BC and ge AE BC for the two signatures of the coupled band, and AE BC gf for band AE. The use of quasiparticle labels, though, cannot be justified for both bands which are obviously quite different. In the AEBC band the two quasiprotons align their angular momenta along the rotation axis at high spin, as expected from the UC calculations in which principal axis cranking (PAC) is realized. In the high- $K$  band the quasiprotons must be coupled mainly to the deforma-

tion axis. The high- $K$  band is not a solution expected from PAC calculations. The high spin parts of the two bands therefore realize different couplings of particles in identical orbitals. These couplings apparently result in a difference in aligned angular momentum of  $\sim 2.5\hbar$ , see fig. 8. The two bands cannot be compared at identical spins, but a linear extrapolation of the energy for the coupled band, which may be justified from the constant alignment above  $\hbar\omega \approx 0.34$  MeV, shows a preference of a few hundred keV for the rotation aligned coupling, see fig 12.

We believe that this case of co-existing coupling schemes is realized for the first time in six-quasiparticle bands. The four neutrons are most likely spectators, and the difference is to be traced to the coupling of the two protons. There is probably a resemblance to the cases of s- and t-bands representing aligned and tilted coupling of the  $i_{13/2}$  quasineutrons in some neutron-rich rare-earths nuclei [17]. The present rather exotic case of six-quasiparticle bands calls for more advanced theoretical considerations.

In principle we would also expect to observe other coupled high- $K$  bands, for example bands assigned configurations like (geAF, gfAF) or (geAG, gfAG). In the present experiment two other coupled bands, X1 and X2, have been observed, but due to the lack of spin and parity assignment no configurations have been assigned to these two bands.

## 7 Summary

In the present experiment high spin states in  $^{166}\text{Hf}$  have been studied. Fourteen new single normal-deformed rotational bands have been established of which six form coupled pairs. Four formerly known bands in  $^{166}\text{Hf}$  have been extended to higher spins. Firm spin and parity have been assigned to most of the new bands based on DCO measurements of the decay-out transitions from the various bands. All new bands except for two have been assigned negative parity.

At low spin the bands have been assigned two- or four-quasiparticle configurations. The extensions of three of the previously known bands are proposed to be built upon proton excitations in a mixed crossing involving the proton orbitals  $h_{11/2}, \alpha = -1/2$  (f) and  $h_{9/2}, \alpha = +1/2$  (g). Within the range of 1 MeV above yrast 67% of the expected four-quasineutron bands have been observed. An upper limit over which no rotational bands have been observed seems to be present. No structures involving more than six quasiparticles (two quasiprotons and four quasineutrons) at high spin have been found. Therefore the placement of this boundary is probably determined by the onset of proton excitations.

One formerly known, now extended, band and one new observed coupled band in  $^{166}\text{Hf}$  have at high spin been assigned six-quasiparticle configurations involving the orbitals  $\nu[642]5/2^+$ ,  $\nu[651]3/2^+$ ,  $\nu[523]5/2^-$ ,  $\pi[514]9/2^-$  and  $\pi[541]1/2^-$ . In the present work these two bands have been proposed to represent the two different coupling schemes, rotation and deformation alignment, built on identical orbitals at high spin, respectively. These

two couplings result in a difference in excitation energy of a few hundred keV between the two bands at high spin, favouring the rotation aligned band. A difference of  $\sim 2.5\hbar$  in aligned angular momentum has also been observed. We believe that co-existing coupling schemes in six-quasiparticle structures involving identical orbitals at high spin have been reported here for the first time.

This work has been supported by the Danish Natural Science Foundation and the EU LSF (contract no. ERB FMGECT 980110). AM acknowledges the partial financial support from the Polish Scientific Committee (KBN Grant No. 2 P03B 001 16). BMN acknowledges support from the Hungarian Scientific Research Fund, OTKA (contract no. T20655 and T32910). The Bonn group acknowledges the support by BMBF (contract no. 06BN815).

## References

1. K.P. Blume, H. Hübel, M. Murzel, J. Recht, K. Theine, H. Kluge, A. Kuhnert, K.H. Maier, A. Maj, M. Guttormsen, A.P. de Lima. Nucl. Phys. A **464**, 445 (1987).
2. <http://www.matfys.lth.se/~ragnar/ultimate.html>.
3. J. Eberth, Prog. Part. Nucl. Phys. **28**, 495 (1992); J. Eberth *et al.*, Nucl. Instrum. Methods A **369**, 135 (1996).
4. G. Duchene *et al.*, Nucl. Instrum. Methods A **432**, 90 (1999).
5. D.C. Radford, Nucl. Instrum. Methods A **361**, 297 (1995).
6. M. Palacz, Nucl. Phys. A **625**, 162 (1997).
7. A. Krämer-Flecken, T. Morek, R.M. Lieder, W. Gast, G. Hebbinghaus, H.M. Jäger, W. Urban, Nucl. Instrum. Methods A **275**, 333 (1989).
8. A. Bohr, B.R. Mottelson, *Nuclear Structure*, Vol. **2** (W.A. Benjamin, New York, 1975).
9. F. Dönau, Nucl. Phys. A **471**, 469 (1987).
10. B.E. Chi, Nucl. Phys. A **83**, 97 (1966).
11. W. Nazarewicz, M.A. Riley, J.D. Garrett, Nucl. Phys. A **512**, 61 (1990).
12. S. Raman, C.H. Malarkey, W.T. Milner, C.W. Nestor, P.H. Stelson, Atom. Nucl. Data Tables **36**, 1 (1987).
13. M. Neffgen, E.M. Beck, H. Hübel, J.C. Bacelar, M.A. Deleplanque, R.M. Diamond, F.S. Stephens, J.E. Draper, Z. Phys. A **344**, 235 (1993).
14. M.B. Smith, G.J. Campbell, R. Chapman, P.O. Tjøm, R.A. Bark, G.B. Hagemann, N. Keeley, D.J. Middleton, H. Ryde, K.-M. Spohr, Eur. Phys. J. A **6**, 37 (1999).
15. J.M. Espino, G.B. Hagemann, I.G. Bearden, R.A. Bark, M. Bergström, A. Bracco, B. Herskind, H.J. Jensen, S. Leoni, C. Martínez-Torre, B. Million, P.O. Tjøm, Nucl. Phys. A **640**, 163 (1998).
16. A. Nordlund, R. Bengtsson, P. Ekström, M. Bergström, A. Brockstedt, H. Carlsson, H. Ryde, Y. Sun, A. Atac, G.B. Hagemann, B. Herskind, H.J. Jensen, J. Jongman, S. Leoni, A. Maj, J. Nyberg, P.O. Tjøm, Nucl. Phys. A **591**, 117 (1995).
17. C.J. Pearson, P.M. Walker, C.S. Purry, G.D. Dracoulis, S. Bayer, A.P. Byrne, T. Kibédi, F.G. Kondev, T. Shizuma, R.A. Bark, G. Sletten, S. Frauendorf, Phys. Rev. Lett. **79**, 605 (1997).